Revised manuscript submitted to *Polymer* for publication, December 2003

CHROMATOGRAPHIC ESTIMATION OF FILLER SURFACE ENERGIES AND CORRELATION WITH PHOTODEGRADATION OF KAOLIN FILLED POLYETHYLENE

Deeba M. Ansari [a, b] and Gareth J. Price[a]*

[a.] Department of Chemistry, University of Bath, Claverton Down, BATH, BA2 7AY, U.K.

and

[b.] Imerys Minerals Ltd., Central Laboratories, Par Moor Road, St Austell, Cornwall, PL24 2SQ, UK

* To whom correspondence and proofs should be addressed. E-mail: g.j.price@bath.ac.uk

---

ABSTRACT

Inverse gas chromatography, IGC, has been used to investigate the surface properties of two calcined kaolins and of polyethylene composites containing calcined kaolin. The results reveal differences in the two kaolins that were not found in XPS spectra nor in their influence on the melting behaviour of the polymer. The kaolin that had a markedly higher surface energy and stronger Lewis acid behaviour was found to shower greater photooxidative degradation in accelerated weathering tests. This novel application of IGC derived surface characterisation of solids further extends the usefulness of the method in this type of work.

Keywords: Inverse Gas Chromatography; Calcined kaolin; surface energy; polyethylene; photo-oxidation

INTRODUCTION

Kaolin, or china clay, is found in many parts of the world and is an important commercial product [1]. Among its uses is as a mineral additive in a range of polymer composite materials. For many applications, the kaolin has to be modified, for example by coating with a modifying agent or being subjected to heat treatment. Calcined kaolins – kaolins that have been heated to > 1000 ºC for an extended period of time - are added to polyethylene (PE) agricultural films to improve their infra red barrier properties [2]. However, addition of such minerals may reduce the lifetime of the polymer films by catalysing photo-oxidation and degradation or by inhibiting the action of stabiliser systems [3], if insufficiently stabilised. These effects, in addition to factors related to film preparation and processing, are critically related to the surface chemistry of the filler so that an understanding of the interactions between the polymer and the kaolin is important for predicting composite performance.

One technique that has found extensive use in studying the properties of solid surfaces and their interactions with polymers is inverse gas chromatography, IGC. Previous work has demonstrated its utility in characterising kaolins and their chemical modifications.

A number of workers have demonstrated the usefulness of IGC for investigating the surface energies of a range of mineral solids[4, 5]. Small amounts of "probe" solvents are injected into a flow of carrier gas over the material under investigation and the retention time depends on the interactions between the probe and the surface. By using probes with a range of properties, the nature of the surface can be defined with good accuracy. The technique has been applied to the measurement of a number of physicochemical properties of a range of polymers[4, 6, 7]. Some of the earliest reports of the use of IGC involved the measurement of crystallinity in polyethylene. [8-10] More recently it has been used to investgate the modification of fillers used in polymer blends involving polyethylene[11,12] as well as the solution thermodynamic[13] and surface[14] properties of the polymer.

IGC been used to characterise a varied range of solid surfaces including silicas[15], activated carbons [16], filler materials and pigments [17-19] and pharmaceutical agents [20,21]. IGC studies of a number of different clay minerals have also been reported. Bandosz *et al*.[22] studied the effect of introducing metal cations into pillared smectites. Alkane and alkene probes were used to show that, after calcination, the Lewis acid sites were reduced with lower π-bonding interactions. The study was extended[23] to include surface polymerisation and carbonisation as well as [24] the effect of heat treatment or high temperature reaction with propylene on taeniolites. In other work, montmorillonite and bentonite [25] matrices were also modified by a similar technique and the sorption properties of the surfaces characterised. The surface properties of illites (another 2:1 clay) and kaolinites this type of clay from various origins were measured by IGC and the use of branched alkane probes allowed characterisation of the surface morphology [26]. This [27] was later extended to use a finite concentration technique to characterise the heterogeneity of the clay surfaces. Thus, the technique is well suited to the studies involved here.

In the work described here, two commercial grades of calcined kaolin have been characterised by IGC and compounded into polyethylene composites. The filled polymers were also studied by IGC and blown films prepared from each material. These were subjected to accelerated weathering and the extent of degradation and changes in some mechanical properties were measured. The results were related to changes in the surface thermodynamic properties of the minerals.

EXPERIMENTAL

Materials: The kaolins were natural kaolins from Imerys Minerals that had been calcined under standard conditions. The compositions of each are detailed in Table 1. The two **CA**lcined **C**lays – termed here CAC1 and CAC2 were from the same feed source, with CAC2 having undergone

a secondary refining process, reducing residual levels of iron, magnesium, titanium and potassium. The polyethylene used was a low density PE (Borealis LE 1870) with a melt flow index of 2.0 and density of 922 kg m^{-3}.

The calcined kaolins were compounded into PE at a loading of 50 wt% with an APV MP2030 twin screw extruder at a die temperature of 180 °C and screw speed of 250 rpm. The masterbatches were dried overnight at 60 °C in a Conair Churchill desiccant dryer. Samples were diluted with the original polymer in a Betol BK 32 film extruder to produce 30 μm thickness films with a 5 wt.% loading of kaolin. Films were also prepared from the virgin polymer as a comparison.

Weathering of polyethylene films: Twelve samples (25 x 150 mm) from each of the three films (PE, PE-CAC1 and PE-CAC2) were subjected to accelerated ageing in a QUV Weatherometer under standard conditions[28] according to ASTM D4392-92 Cycle A. The test method uses UVA-340 lamps with a peak emission at 343 nm, simulating a significant proportion of natural sunlight. A sample of each film was periodically removed and analysed up to two hundred hours exposure time, after which the films had embrittled and lost most of their mechanical strength.

Analytical methods: Scanning electron microscopy (SEM) was performed on a Phillips-Electroscan 2020 SEM which was also used for elemental surface analyses. Thermal transitions for the polymer were measured by differential scanning calorimetry (DSC) with a Perkin-Elmer V1.8TA using a scan rate of 10 °C min^{-1} under a nitrogen atmosphere.

Degradation of the films was monitored by FTIR[29] using a Nicolet Magna-IR 550 spectrometer[30]. The tensile strength and elongation of the films were measured on a Monsanto T10 mechanical tester, with 100N load cell and with a sample size of 25 x 60 mm.

Chromatography: Chromasorb W, AW DMCS treated, 100-120 mesh, was used as an inert support for the PE and filled materials which were coated at a level of 10% w/w from hot AnalR cyclohexane. The exact loading of the stationary phase was determined by repeat calcination at

1000 °C in a CEM AirWave 7000 microwave furnace, accounting for the presence of the kaolins by using data from blank runs. Packings of the calcined kaolins were prepared by compaction under pressure followed by crumbling and sieving to give aggregates of 425 – 850 μm particle size. Stainless steel columns ¼ in o.d. of length 0.90 – 1.0 m were packed with 10-15 g of stationary phase. The columns were connected to the GC and pre-conditioned at 150 °C for 24 hours, before further conditioning for twelve hours at the required temperature.

A Perkin-Elmer Autosystem XL gas chromatograph employing FID detection was used. The column temperature was measured to ± 0.2 °C on a Chrompack RDT thermometer that was calibrated against an NPL calibrated Tinsley Type 5840 platinum resistance thermometer. Looped-valve tubing before the column inlet permitted inlet pressure and flow to be measured to ± 0.3 cm^3 min^{-1} with a FP-407 (Chrompack) solid state calibrated dual flow and pressure meter. Oxygen-free nitrogen was used as the carrier gas and was passed through a Perkin-Elmer three-stage drying and purification system, before entering the chromatograph. Barometric pressure was measured at the beginning and end of each run using a BDH precision aneroid barometer. The mean of the two was used for all calculations. The instrument was located in a temperature-controlled laboratory maintained at 23 °C ± 1 °C.

After conditioning, a series of ~ 0.1μL aliquots of the vapour of the probes used were injected by Hamilton syringe over a range of temperatures. All probes were chromatographic grade (BDH). Retention times were recorded and processed by the PE-Nelson Turbochrom data management software. Methane was used as a non-interacting marker to determine the void volume of the column. Each value reported is the result of at least three elutions agreeing to within experimental uncertainty.

RESULTS AND DISCUSSION

Characterisation of polymers and kaolin surfaces

The primary measurement in IGC is the net retention volume, V_n, given [31] by

$$V_n = J\, f\, (t_r - t_0) \qquad (1)$$

where t_r is the retention time taken for the probe, t_0 that for the non-interacting marker and f is the carrier gas flow rate corrected to standard temperature and pressure and corrected for the pressure drop along the column[31]. J is the correction factor for pressure drop across the column and carrier gas compressibility, given with the column inlet and outlet pressures, p_i and p_o respectively by:

$$J = \frac{3}{2}\left[\frac{(p_i / p_0)^2 - 1}{(p_i / p_0)^3 - 1}\right]$$

In work with polymers[6], it is usual to present the data as a van't Hoff type retention diagram and the data for five alkane probes on PE is shown in Figure 1. The results show the usual shape for the retention diagram of a semi-crystalline polymer[6, 9]. The low temperature linear regions correspond to interaction of the probe only with the amorphous regions and surface of the polymer. The probe does not enter the crystalline regions. In the high temperature region, the probe interacts with the whole polymer sample. The non-linear region corresponds to non-equilibrium retention around a phase transition. In the case of a melting transition, the melting point, T_m is taken as the lowest temperature at which bulk equilibrium sorption takes place i.e. the highest temperature at which crystalline regions exist. The results in Figure 1 show this to be 111 °C. Measurement of T_m by DSC gave a value of 112 ºC confirming the accuracy of the IGC value.

The retention diagrams for the two composite materials are shown in Figures 2 and 3. Although there is rather more scatter and curvature in the data, the melting points are clearly discernable and were also measured to be 110 - 111 °C in each case. Thus, there is no

significant effect of the filler on the melting point of the polymer. There is noticeably more curvature in these plots than in Figure 1, making accurate determination of T_m more difficult. This is caused by the higher enthalpy of interaction introduced by the kaolin (see below) which leads to a larger temperature dependence and hence not strictly linear behaviour.

Below T_m, the slopes of the lines in Figure 1 are given by $-\Delta H^o_s/R$ according to the relation

$$\Delta H_s^\circ = -R\frac{\partial \ln V_n}{\partial\left(1/T\right)} \qquad (2)$$

where ΔH^o_s is the enthalpy of solution of the probe in the amorphous polymer. This comprises the enthalpies of condensation and mixing for the probe-polymer pair. The calculated values for the alkane probes in the homopolymer and the composites are given in Table 2. Also shown are the values for the kaolins used as the fillers, the retention diagrams for these materials being illustrated by that for CAC1 in Figure 4. The retention diagram for CAC-2 was very similar in appearance and showed no remarkable features. These differ from Figures 1 – 3 since there are no phase transitions in the temperature range studied; hence the plots are linear. In addition the retention is solely due to surface interactions so that the enthalpy of adsorption, ΔH_a° is being measured.

The values obtained for PE are low and differ little from the enthalpies of vaporization of the probes which range[32] from 25.8 kJ mol^{-1} for pentane to 34.4 mol^{-1} for octane (these values correspond to the boiling temperatures). As expected, this is an indication that there are no strong interactions in these systems and the enthalpy of mixing is close to zero. The data from the two calcined kaolins, between which there was little difference, show that strong interactions do occur on these surfaces. Previous work[33] has shown that the kaolins retain polar groups on the surface after calcination and these can polarise the alkanes leading to higher enthalpies of adsorption.

The results for the filled materials are intermediate between those of the fillers and the polymer matrix but are closer to the former. In these materials, retention will comprise bulk sorption into the amorphous PE and adsorption onto the filler surfaces. The results obtained are clearly not a weighted average of the two contributions and indicate that interaction of the probes with the kaolin is not completely masked by the PE matrix. Since the probe-PE mixing is athermal, the temperature dependence of retention will be dominated by the enthalpy of condensation and the interaction with the kaolin.

To further characterise the nature of the surfaces, the approach of Balard and co-workers[27] was used to calculate the surface energies. Following the approach pioneered by Fowkes [34] the surface energy of the solid, γ_s can be split into two components, arising from intermolecular dispersion forces, γ_s^d, and one due to other specific interactions, γ_s^{sp}

$$\gamma_s^d = \gamma_s^d + \gamma_s^{sp} \quad (4)$$

The non-specific or dispersive component of the substrate surface energy, γ_s^d, can be calculated from the elution data for alkane vapours, which are assumed to interact only by dispersion interactions. The free energy change for the adsorption of a single methylene group, $\Delta G^\circ_{a,CH_2}$, is found from the difference in free energies of adsorption for succeeding alkanes in an homologous series

$$\Delta G^\circ_{a,CH_2} = -RT\, ln\left(\frac{V_n^\circ(n+1)}{V_n^\circ(n)}\right) \quad (5)$$

where n is the number of carbons in the alkane. γ_s^d can then be calculated from [35, 36]

$$\gamma_s^d = \frac{1\left(-\Delta G_a^{\circ,CH_2}\right)^2}{\gamma_{CH_2}\left(2Na_{CH_2}\right)} \quad (6)$$

where N is Avogadro's number; γ_{CH2} is the surface tension of a hypothetical surface containing only methylene groups and a_{CH2} is the cross-sectional area of a methylene group (≈ 0.06 nm^2). $\Delta G^\circ_{a,CH_2}$ is found at constant temperature from a linear plot for a series of alkane probes of RT *ln*

(V_n) *versus* the number of carbon atoms. An example of the plots is shown in Figure 5. The plots for the other system were similar; all the systems showed the expected linear relationship and calculated values of γ_s^d are given in Table 3.

The γ_s^d results for CAC1 and CAC2 were considerably higher than the polymer, again reflecting the polar nature of the kaolin surface. Results for CAC2 were between 5 to 20 mJ m^{-2} lower than those for CAC1, considered significant in terms of the uncertainty of the measurements. These values would suggest that CAC1 has the more polar and hence reactive surface. The results for PE are in good agreement with published data[37] for the surface free energy for polyethylene of 31 mJ m^{-2}. It should be noted that in this case, the values are strictly not those of γ_s^d. Here, the differences in retention between successive alkanes will represent the increment in the free energy of solution. However, in the alkane systems, the athermal mixing means that the values are all similar. However, such an approach would not be valid for polymers with significant enthalpies of mixing. The same comments can be applied to the composite materials where again the surface free energy contribution was dominated by absorption into polyethylene.

To investigate the differences between the two kaolins, SEM micrographs of the filled composites were recorded, those for CAC1 being shown in Figure 6. The images of the materials revealed a rough surface, giving the appearance of having the calcined kaolin particles encapsulated in the polymer matrix. There were no visible differences between films containing the two fillers. From the XPS analysis of the materials illustrated in Figure 7, the surfaces comprised a large proportion of silicon and aluminium, as would be expected from a calcined kaolin, the PE being shown by the large carbon peak. Importantly, no significant differences were seen between the two composites.

The nature of the interactions at the kaolin surfaces were further characterised by using non-alkane probes to estimate specific interactions and hence γ_s^{sp}. Saint-Flour and Papirer [38, 39]

suggested that a plot of ΔG^{o}_{a} as a function of the saturated vapour pressure of alkane probes should give a straight line which could act as a standard, deviation from which gives a measure of the specific interactions for other probes. A number of workers have used this approach and demonstrated its usefulness and equivalence to more thermodynamically rigorous treatments. In this work, the results will be used qualitatively as a comparison of the two systems; quantitative application of the concepts is more subject to interpretation.

From the retention volumes for probes on PE at 100 ºC, Figure 8 was constructed and specific interactions, γ_s^{sp} were calculated and are shown in Table 4. Also indicated is the nature of the probe in terms of its acid-base character as well as the data for the two kaolins illustrated for CAC2 in Figure 9.

As PE is non-polar and can be considered to be chemically inert, no significant polar interactions would be expected. This is reflected in the results in Table 5 where the interaction energies range from –2.7 kJ mol^{-1} for acetone to + 0.9 kJ mol^{-1} for THF. There is no correlation of acidic and basic probes deviating above or below the line indicating that the surface is essentially neutral in these respects.

Kaolin surfaces are known to be acidic and this is also reflected in the results in Table 4. No elution peaks could be detected for strongly basic probes due to their strong interaction with the surface, the probes possibly becoming bound irreversibly or the peaks being so broad as to be unquantifyable. The strongly acidic probe, methanol, could not be detected, although carbon tetrachloride interacted weakly, with the datapoints falling below the alkane line. Cyclohexane was eluted to determine the accessibility of the surface to a bulky probe species, the similarity of the results for CAC1 and CAC2 indicating similar accessibility and porosity. For CAC2, the interactions were 20 – 30% lower than CAC1. It is also noteworthy that the acetone probe was detected after elution from CAC2, but was not detected for CAC1. These results suggest therefore that both kaolins have polar surfaces, primarily acidic in nature

but that CAC1 is the more acidic of the two. There are negative apparent interaction energies for cyclohexane and carbon tetrachloride with the clays, implying lower interaction than with the corresponding alkane. In the former case, the nature of the interactions interactions would be the same and the lower value is presumably due to steric factors preventing the bulkier cyclohexane from accessing sites that are available to the linear compound. The same argument can be made for the relatively bulky CCl_4 probe. Thus the results for these probes may reflect changes in the morphology of the surface in addition to changes in its chemical nature. The degree of porosity and/or intercalation would be lower in the treated clays. Depending on its orientation at the surface, chloroform could also present a surface area similar to that of CCl_4.

Thus, IGC detected differences in the surface properties of the two kaolins even though they could not be differentiated by XPS. It was therefore of interest to determine whether these differences would affect the performance of the composites in use.

Weathering of polyethylene and composite films

Blown films prepared from the two composite materials and from the unfilled PE were exposed to accelerated aging. Unlike films in commercial applications, no stabilisers were added. To investigate the change in mechanical properties, the elongation at break was measured as a function of exposure time, the results being shown in Figure 10.

After an initial increase due to chain relaxation during heating in the weatherometer, all the samples showed reduced elongation at break until 200 hr weathering after which time they were brittle and had lost mechanical integrity. This is a result of degradation of the polymer structure, in particular chain breakage and reduction in molecular weight[40]. However, there were clear differences between the films. Both filled materials degraded faster than the parent polymer; the composite with CAC1 degraded faster than that with CAC2.

These results were mirrored by FTIR measurements on the films. The presence of carbonyl functionality in the polymer is an indicator of oxidation due to PE chain degradation [40-

[42]. The growth of the peak 1715 cm^{-1} in the infra-red spectra of the films is shown in Figure 11. The rate of degradation shown by this indicator again follows the trend PE-CAC1 > PE-CAC2 > PE.

Further discussion

Both the change in mechanical properties and the extent of polymer oxidation showed that PE containing CAC1 was less stable to UV photooxidation than films containing the CAC2 filler. Both composites were less stable than the parent homopolymer. XPS spectra indicated no differences between the two kaolins and neither was found to influence the crystallisation behaviour of the polymer. However, IGC was able to distinguish clear differences between the surface properties of the two minerals. CAC1 was found to have a higher dispersive component of the surface free energy indicating that some sites of higher energy were present. These were shown by the use of probes with varying donor-acceptor character to give CAC1 a more acidic surface than CAC2.

These polar sites must therefore be influential in catalysing UV photo-oxidation and degradation. The carbonyl functionality arises in the degraded polymers as a result of radical chain reactions causing C-H and C-C bond breakage followed by oxidation[40, 43]. The presence of trace metals and chemical irregularities in the polymer chain formed during fabrication and processing acts as initiation centres for photo-oxidation. Reactive sites at filler surfaces also enhance UV absorption and the formation of reactive intermediates. In this regard, the slightly higher proportion of heavy metals in CAC1 compared with CAC2 may be significant. However, they do not completely explain the results.

The findings here support the work of Hancock et al.[44] who compared the photo-degradability of stabilised polyethylene films containing hydrous kaolins and calcined kaolins. Films containing hydrous kaolins degraded significantly faster than those containing calcined kaolins, even though the two kaolins had comparable levels of heavy metals, known to catalyse

photo-oxidation. These differences were attributed primarily to the number of surface active Lewis acid sites, rather than the presence of heavy metals. In previous work[33] we have shown that the hydrous kaolins from which CAC1 and CAC2 were derived have a significantly higher γ_s^d, are more polar have a higher surface acidity than the calcined materials. Thus, the presence of Lewis acid sites at the surface appears to play a significant part in the susceptibility of kaolin-filled PE films to photooxidation.

In contrast to the films studied here, in commercial applications correctly formulated stabiliser systems are added to the films to prolong in-service lifetimes and multiseason films are in common use throughout Europe. Studies using flow microcalorimetry on LDPE films with silica additives[45] showed the interactions between all the components are complex but are influenced by the surface area and porosity and also by surface chemistry in terms of hydrophilicity and surface energy. IGC can be used to investigate interactions in multicomponent systems and may have a part to play in further characterising these polymer composite systems. In addition, the surface properties of the kaolins are important in determining the mechanical properties of the polymeric films and these are also amenable to study by IGC. The model used here is relatively simple and more sophisticated versions are available which allow more detailed interpretation of molecular behaviour at surfaces [46 – 48]. However, even with the straightforward model employed here, the utility of IGC to distinguish between solid surfaces is clear.

CONCLUSIONS

The results described here further reinforce the application of IGC in characterising the surfaces of fillers in polymer systems. Differences between the surface properties of two calcined kaolins were determined despite the similarity of their crystallisation behaviour and their XPS spectra. The kaolin with the markedly higher surface energy and stronger Lewis acid behaviour was

found to shower greater photo-oxidative degradation in accelerated weathering tests. Further work is now in progress to establish a firm correlation between surface energy and photochemical behaviour. This may be used for commercial improvements for such additives in the near future. Thus, the work illustrates another potential use of IGC in predicting the behaviour and performance of polymer composites.

REFERENCES

1. R. E. Grim *Clay Mineralogy*. Mcgraw-Hill, New York (1968)
2. M. Hancock *Plasticulture* 79, 4 (1998).
3. L. Achimsky, L. Audouin and J. Verdu *Polym. Degrad. Stabil.* 57, 231 (1997).
4. D. R. Lloyd, T. C. Ward and H. P. Schreiber (Eds) *Inverse Gas Chromatography: Characterisation Of Polymers And Other Materials*, Amer. Chem. Soc., Washington DC, (1989)
5. D. R. Williams *Chromatography And Analysis* 2, 9 (1991).
6. Z. Y. Al-Saigh and J. E. Guillet (2000). Inverse Gas Chromatography In The Analysis Of Polymers and Rubbers In R. Meyers (Ed), *Encyclopedia Of Analytical Chemistry: Instrumentation And Applications*, Wiley, Pp. 7759
7. R. P. Danner, F. Tihminlioglu, R. K. Surana and J. L. Duda *Fluid Phase Equilib.* 148, 171, (1998).
8. O. Smidsrod and J. E. Guillet *Macromolecules* 2, 272, (1969).
9. D. G. Gray and J. E. Guillet *Macromolecules* 6, 223, (1973).
10. J. E. Guillet, M. Romansky, G. J. Price and R. Van Der Mark (1989). in D. R. Lloyd, T. C. Ward And H. P. Schreiber (Eds), *Inverse Gas Chromatography: Characterisation Of Polymers And Other Materials*, Amer. Chem. Soc., Pp. 20
11. W.D. Wang, H. Liang, B.D. Favis and H.P. Schreiber, *J. Appl. Polym. Sci.* 81, 1891(2001)
12. N. Ljungqvist, T. Hjertberg, A.L. Persson and H. Bertilsson. *Composite Interfaces* 5, 11 (1997)
13. L. Zhao and P. Choi. *Polymer* 42, 1075 (2001)
14. P. Uhlmann and S. Schneider *J. Chromatogr. A*, 969, 73 (2002)
15. H. Balard, M. Sidqi, E. Papirer, J. B. Donnet, A. Tuel, H. Hommel And A. P. Legrand *Chromatographia* 25, 707, (1988).

16. E. Papirer, E. Brendle, F. Ozil and H. Balard *Carbon* 37, 1265, (1999).
17. A. Lundqvist and L. Odberg *J. Pulp Pap. Sci.* 23, J298, (1997).
18. H. Balard and E. Papirer *Prog. Org. Coat.* 22, 1, (1993).
19. D. S. Keller and P. Luner *Colloid Surf. A-Physicochem. Eng. Asp.* 161, 401, (2000).
20. B. C. Hancock and S. L. Shamblin *Pharm. Sci. Technol.* 1, 345, (1998).
21. M. D. Ticehurst, R. C. Rowe and P. York *Int. J. Pharm.* 111, 241, (1994).
22. T. J. Bandosz, J. Jagiello, B. Andersen and J. A. Schwarz *Clay Min.* 40, 306, (1992).
23. T. J. Bandosz, J. Jagiello, K.A. Amankwah and J. A. Schwarz *Clay Min.* 27, 435, (1992).
24. T. J. Bandosz, J. Jagiello and J. A. Schwarz *J. Chem. Soc.-Faraday Trans.* 92, 4631, (1996).
25. B. Hamdi, Z. Kessaissia, J. B. Donnet and T. K. Wang *Ann. Chim.-Sci. Mat.* 24, 63, (1999).
26. A. Saada, E. Papirer, H. Balard and B. Siffert *J. Colloid Interface Sci.* 175, 212, (1995).
27. H. Balard, A. Saada, E. Papirer and B. Siffert *Langmuir* 13, 1256, (1997).
28. ASTM *Standard Practice For Operating Light And Water Apparatus For Exposure Of Plastics* (1992).
29. A. Davis and D. Sims *Weathering Of Polymers*. Elsevier, London (1986)
30. H. Al-Madfa, Z. Mohamed and M. E. Kassem *Polymer Degradation And Stability* 62, 105 (1998).
31. J. R. Conder and C. L. Young *Physicochemical Measurement By Gas Chromatography*. Wiley, New York (1978)
32. R. Weast (Ed) *Handbook Of Chemistry And Physics*, Chemical Rubber Co., 81st Edn (2001)
33. D. M. Ansari and G. J. Price *Submitted For Publication* (2003).
34. F. M. Fowkes *Ind. Eng. Chem. Prod. Res. Dev.* 56, 40, (1967).
35. F. M. Fowkes (1991). in K. L. Mittal and H. R. Anderson (Eds), *Acid-Base Interactions: Relevance To Adhesion Science And Technology*, VSP, p. 93
36. J. H. Park, Y. K. Lee and J. B. Donnet *Chromatographia* 33, 154, (1992).
37. D. H. Kaelble *Physical Chemistry Of Adhesion*. Wiley Interscience, Chichester (1970)
38. C. Saint-Flour and E. Papirer *Ind. Eng. Chem. Prod. Res. Dev.* 21, 666, (1982).
39. C. Saint-Flour and E. Papirer *Ind. Eng. Chem. Prod. Res. Dev.* 21, 337, (1982).
40. G. Scott (Ed) *Mechanisms Of Polymer Degradation And Stabilisation*, Elsevier, London, (1990)

41. P. Gijsman and A. Dozeman *Polym. Degrad. Stabil.* 53, 45, (1996).

42. P. Gijsman, G. Meijers and G. Vitarelli *Polym. Degrad. Stabil.* 65, 433, (1999).

43. P. A. Dilara and D. Briassoulis *Polymer Testing* 17, 549 (1998).

44. M. Hancock, J. E. Marsh and R. L. Lee *Filplas '92. Manchester*. (1992)

45. N. S. Allen, M. Edge, T. Corrales, A. Childs, C. M. Liaw, F. Catalina, C. Peinado, A. Minihan and D. Aldcroft *Polym. Degrad. Stabil.* 61, 183 (1998).

46. J.B. Donnet, S.J. Park and H. Balard *Chromatographia* 31, 434 (1991)

47. E. Brendle and E. Papirer *J. Colloid Interface Sci*. 194, 207 (1997)

48. E. Brendle and E. Papirer *J. Colloid Interface Sci*. 194, 217 (1997)

Table 1: Physical and chemical properties of calcined clays

		CAC1	CAC2
ISO brightness		88.8	92.0
ECC yellowness		4.9	4.6
BET surface area		7.0	7.1
Particle size (wt.%)	> 10 μm	5	6
	> 5 μm	15	17
	< 2 μm	49	49
	< 1 μm	12	12
	< 0.5 μm	< 5	6
	< 0.25 μm	< 5	< 5
Composition	SiO_2	55.8	55.9
	Al_2O_3	41.0	41.5
	Fe_2O_3	0.59	0.41
	TiO_2	0.06	0.02
	CaO	0.01	0.02
	MgO	0.19	0.11
	K_2O	2.21	1.90
	Na_2O	0.01	0.01
	Loss on ignition	0.30	0.20

Table 2: Isosteric enthalpies of interaction for n-alkanes on PE, clay fillers and clay-filled PE composites

	Enthalpy of Interaction (kJ mol^{-1})				
Probe	**PE[1]**	**CAC1[2]**	**CAC2[2]**	**PE-CAC1 composite[3]**	**PE-CAC2 composite[3]**
Pentane	24 ± 2	38 ± 2	39 ± 4		
Hexane	27 ± 2	48 ± 3	46 ± 2		
Heptane	25 ± 2	62 ± 2	61 ± 2	52 ± 3	49 ± 2
Octane	31 ± 1	79 ± 2	70 ± 3	59 ± 2	58 ± 3
Nonane	31 ± 2			62 ± 3	60 ± 2
Decane	34 ± 2			66 ± 2	63 ± 2

[1] Enthalpy of solution;

[2] Enthalpy of adsorption;

3 Enthalpy of solution + adsorption.

Table 3: Dispersive component of surface free energy data for fillers and filled PE's

	Dispersive component of surface free energy (mJ m^{-2})				
Temperature (ºC)	**CAC1**	**CAC2**	**PE-CAC1 composite**	**PE-CAC2 composite**	**PE**
80	139 ± 4	128 ± 4	32 ± 1	30 ± 2	33 ± 1
90	137 ± 5	117 ± 4	32 ± 2	33 ± 1	32 ± 2
100	132 ± 4	115 ± 3	34 ± 2	35 ± 2	
110	126 ± 4	111 ± 5	36 ± 2	32 ± 1	
120	130 ± 3	113 ± 4	34 ± 1	33 ± 2	
130	124 ± 2	111 ± 3	33 ± 1	35 ± 2	
140	113 ± 2	108 ± 4	36 ± 2	34 ± 1	

Table 4: Specific interaction data for PE at 100 ºC.

	Specific interaction $-\Delta G_{specific}$ (kJ mol^{-1})			
Probe	**PE**	**CAC1**	**CAC2**	**Probe character**
Acetic acid	-1.3 ± 1.2			Strong acid
Chloroform	0.1 ± 1.1			Weak acid
Carbon tetrachloride	0.8 ± 1.3	-2.7 ± 0.9	-2.1 ± 0.6	Weak acid
Cyclohexane	0.6 ± 1.5	-4.3 ± 1.1	-3.8 ± 1.0	Non-polar
Acetone	-2.7 ± 1.6	NPD	1.0 ± 0.4	Amphoteric
Hexene	-1.4 ± 0.9	4.0 ± 0.9	3.4 ± 0.6	Weak base
Octene	-2.1 ± 1.2	3.8 ± 0.7	3.0 ± 0.9	Weak base
Toluene	0.7 ± 1.0			
THF	0.9 ± 0.8	NPD	NPD	Base
Pyridine	-1.9 ± 1.4	NPD	NPD	Strong base

CAPTIONS FOR FIGURES

Figure 1: van't Hoff retention diagram for alkanes on PE.

Figure 2: Retention diagram for CAC1 – PE composite.

Figure 3: Retention diagram for CAC2 – PE composite.

Figure 4: Retention diagram for CAC1.

Figure 5: Plot of ΔG_a versus T for CAC1.

Figure 6: SEM images of the PE-CAC1 composite material.

Figure 7: XPS spectra of the filled PE-CAC composites

Figure 8: Plot of ΔG_a versus log P_o for PE.

Figure 9: Plot of ΔG_a versus log P_o for CAC2.

Figure 10: Peak elongation versus weathering time for PE films.

Figure 11: Area under the carbonyl peak in the FTIR spectra versus weathering time for PE films.

Figure 1: van't Hoff retention diagram for alkanes on PE.

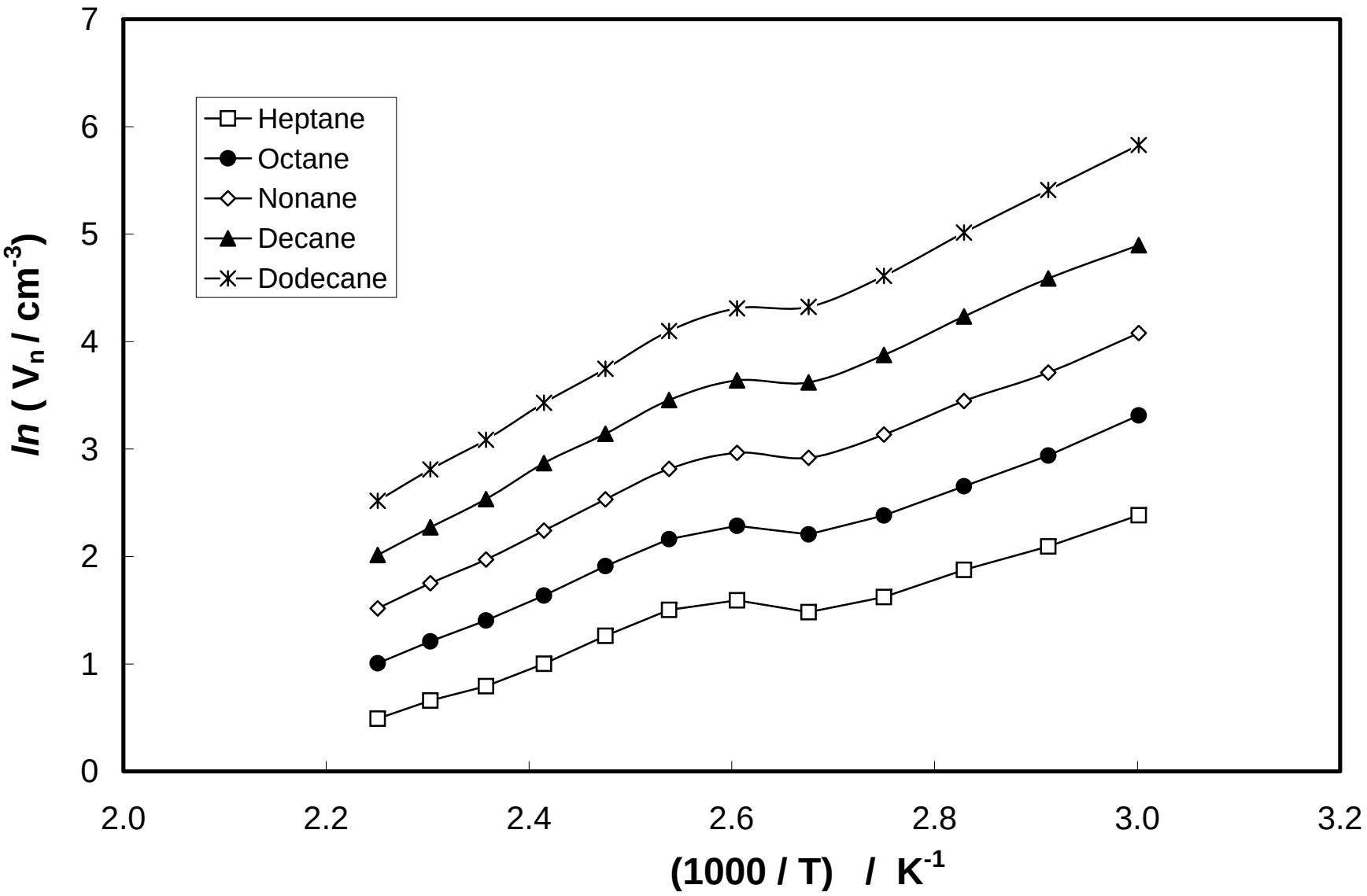

Figure 2: Retention diagram for CAC1 – PE composite.

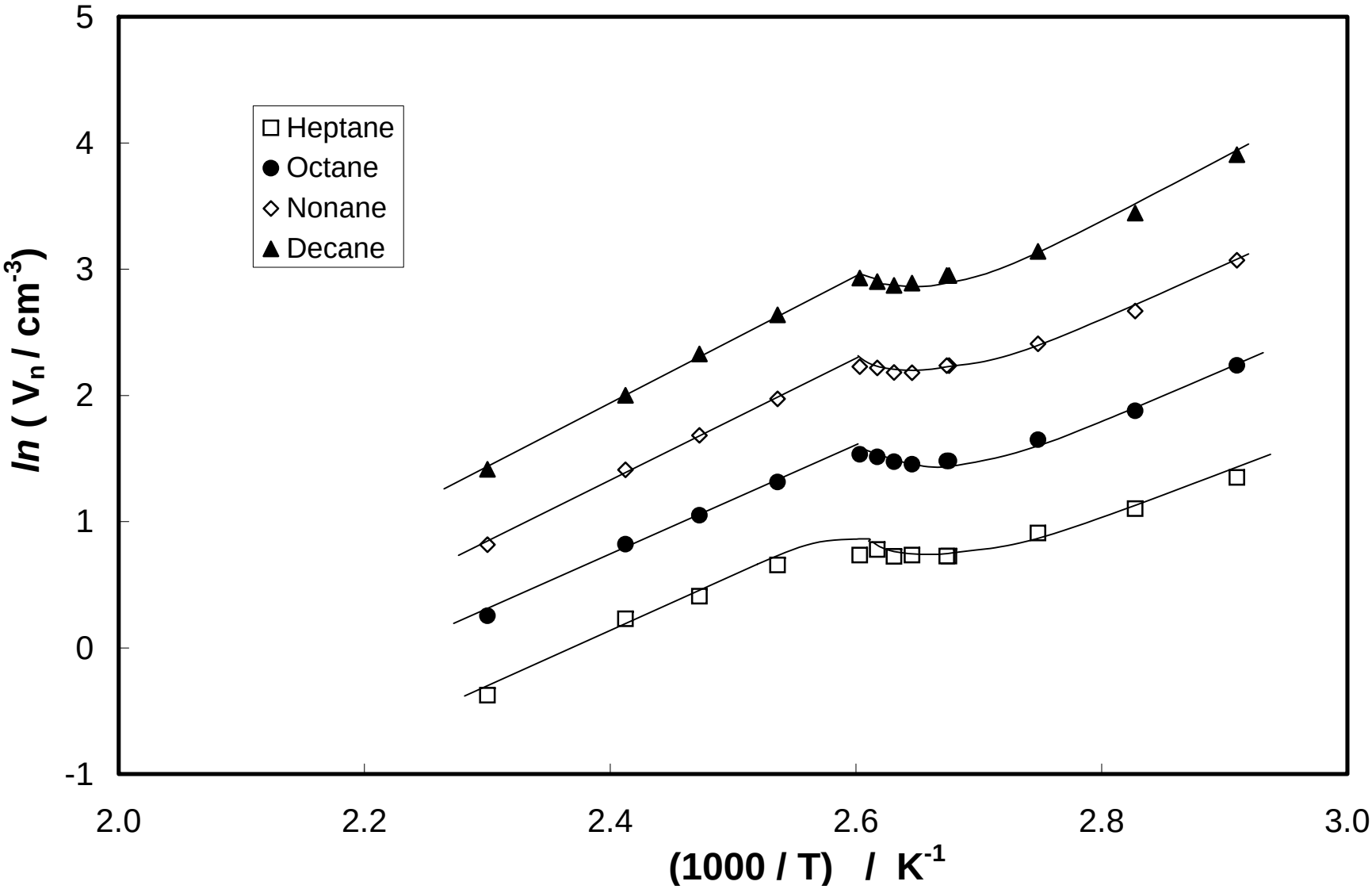

Figure 3: Retention diagram for CAC2 – PE composite.

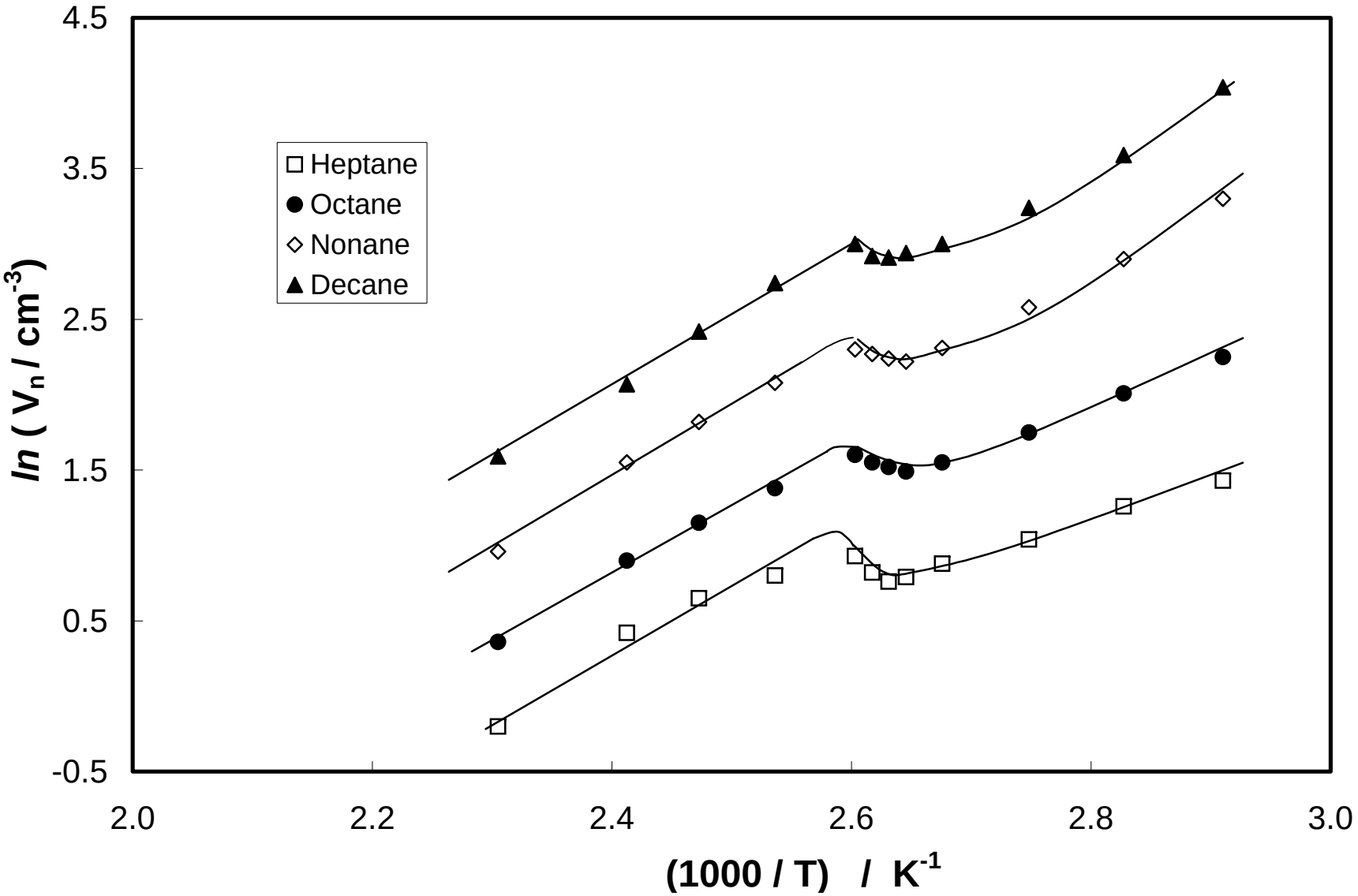

Figure 4: Retention diagram for CAC1.

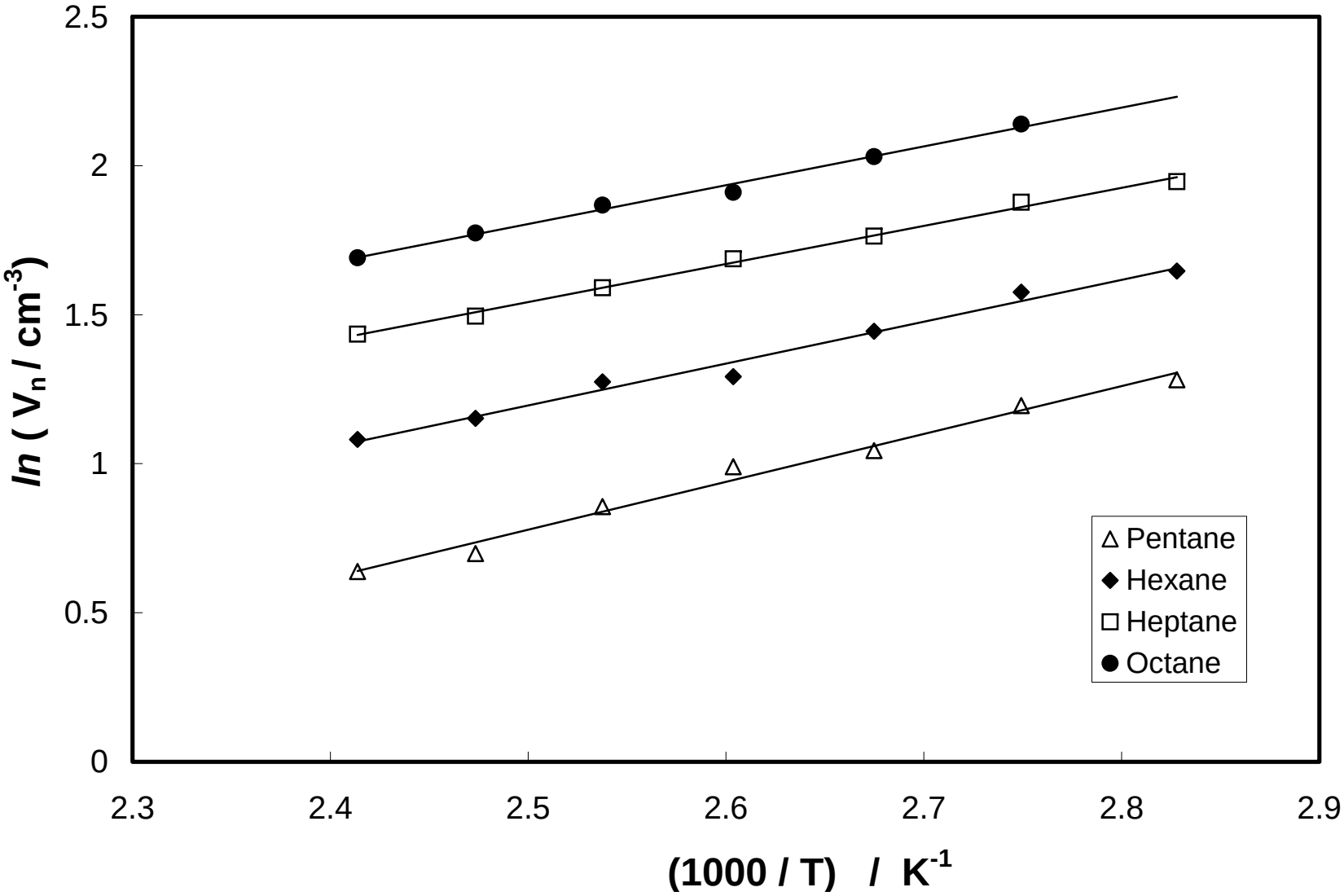

Figure 5: Plot of ΔG_a versus T for CAC1.

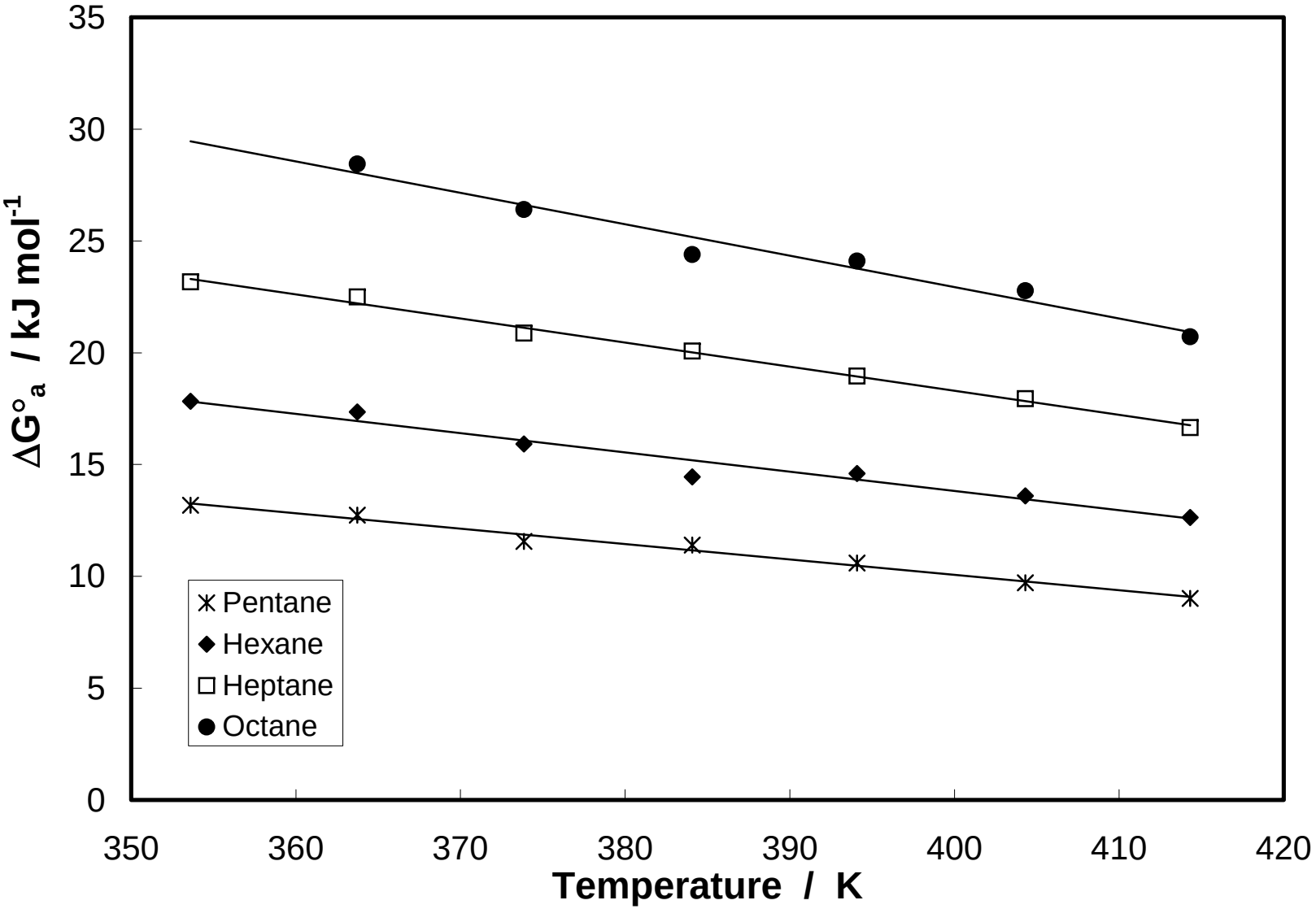

Figure 6: SEM images of the PE-CAC1 composite material.

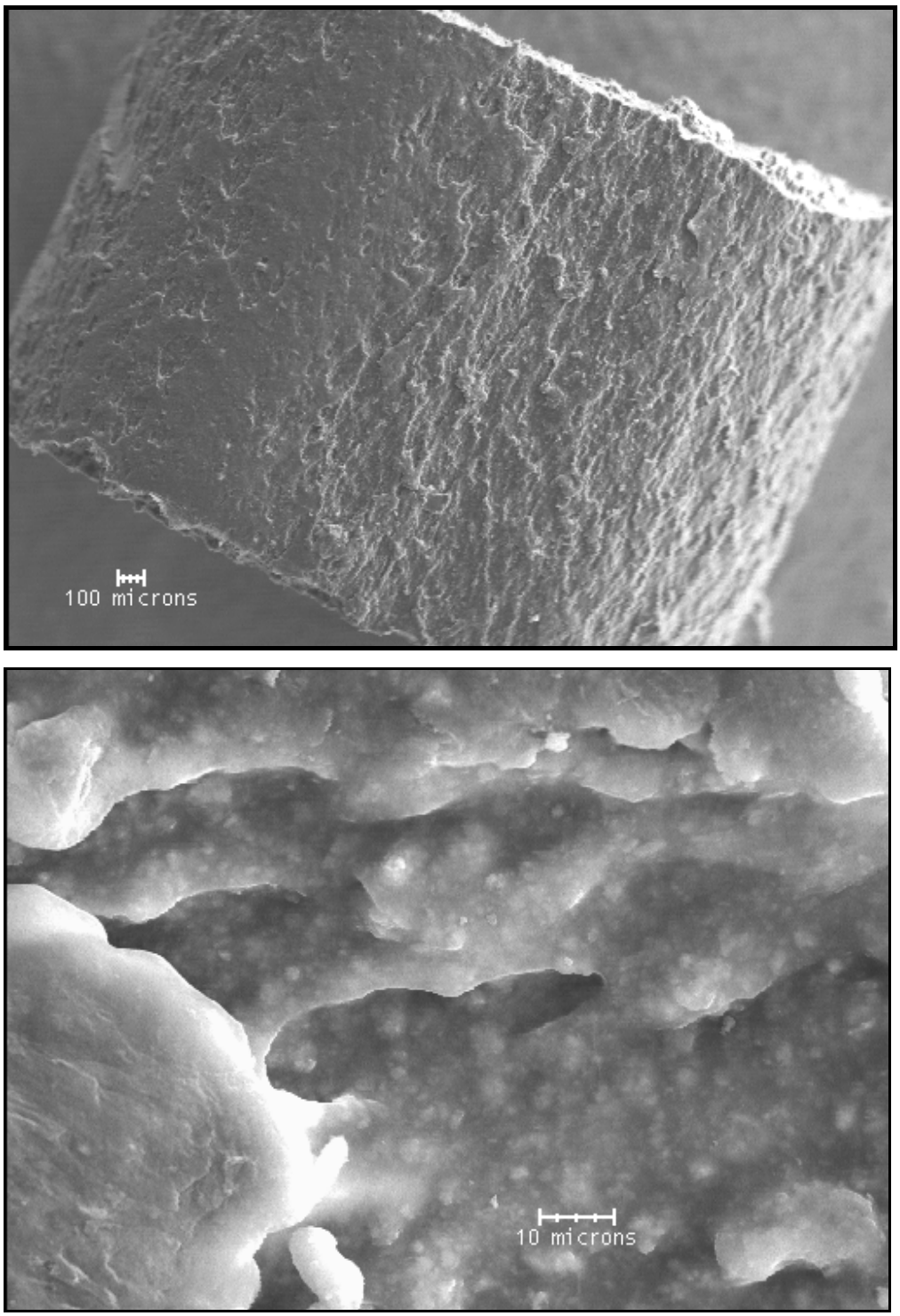

Figure 7: XPS spectra of the filled PE-CAC composites

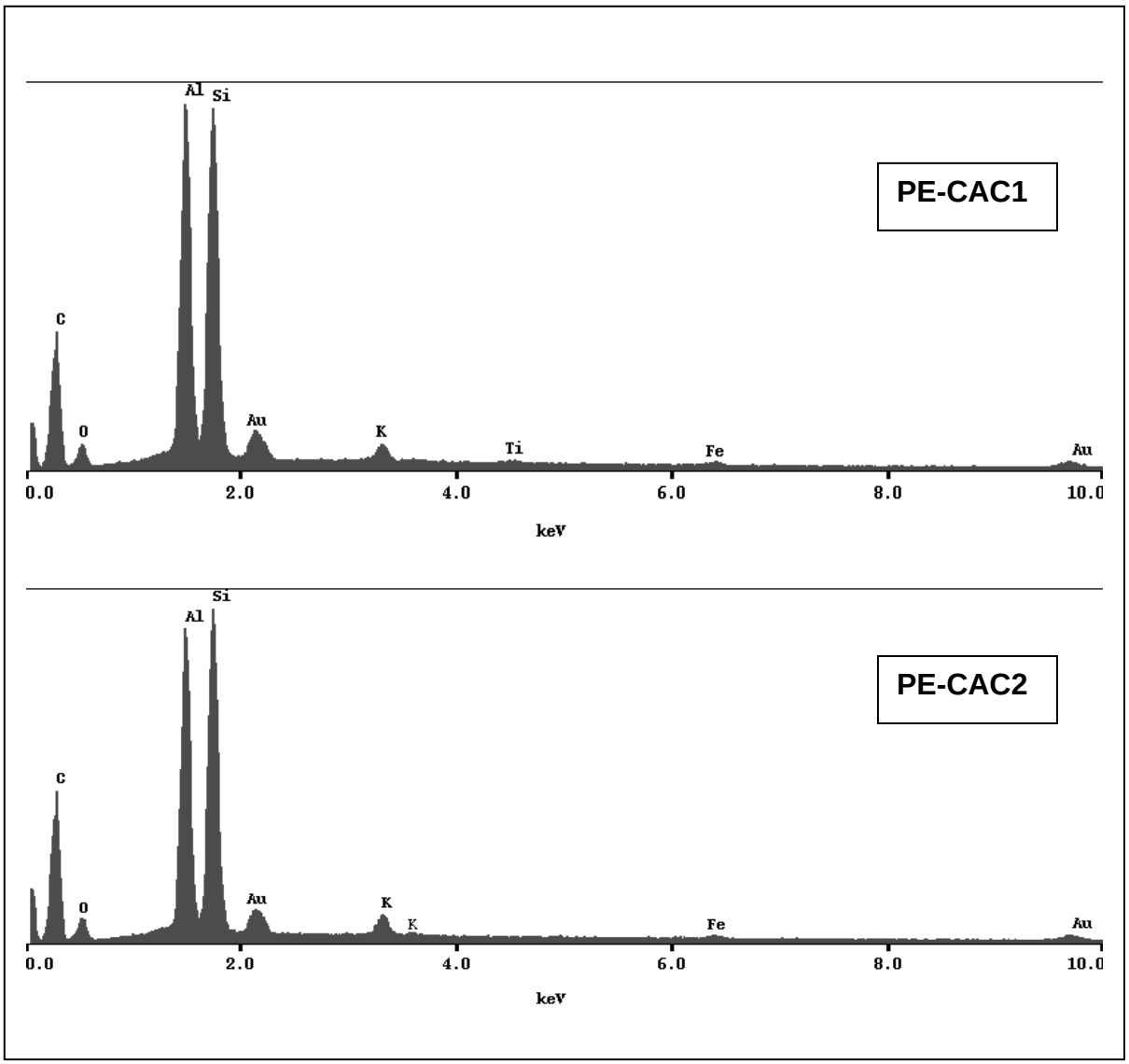

Figure 8: Plot of ΔG_a versus log P_o for PE.

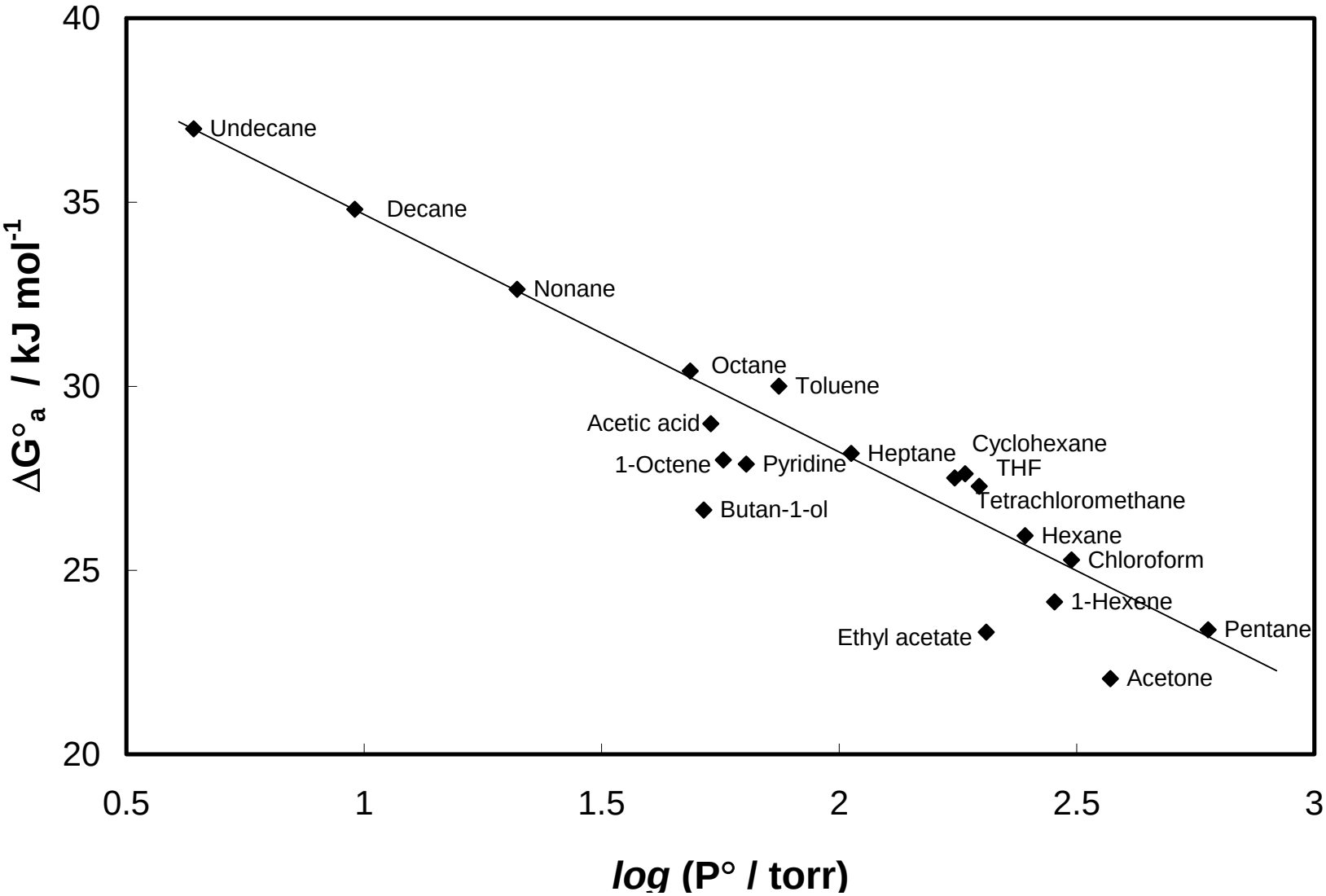

Figure 9: Plot of ΔG_a versus log P_o for CAC2.

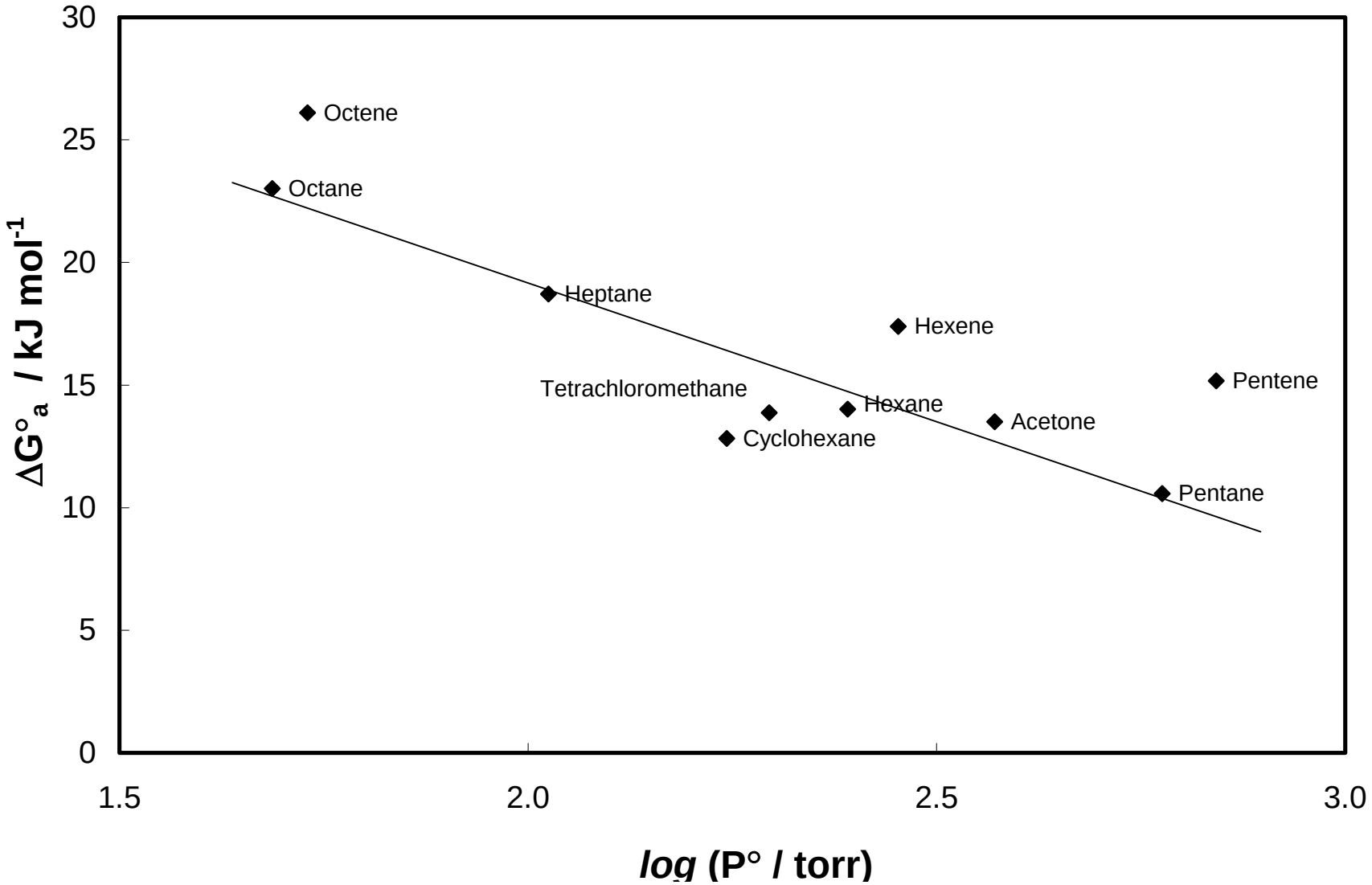

Figure 10: Peak elongation versus weathering time for PE films.

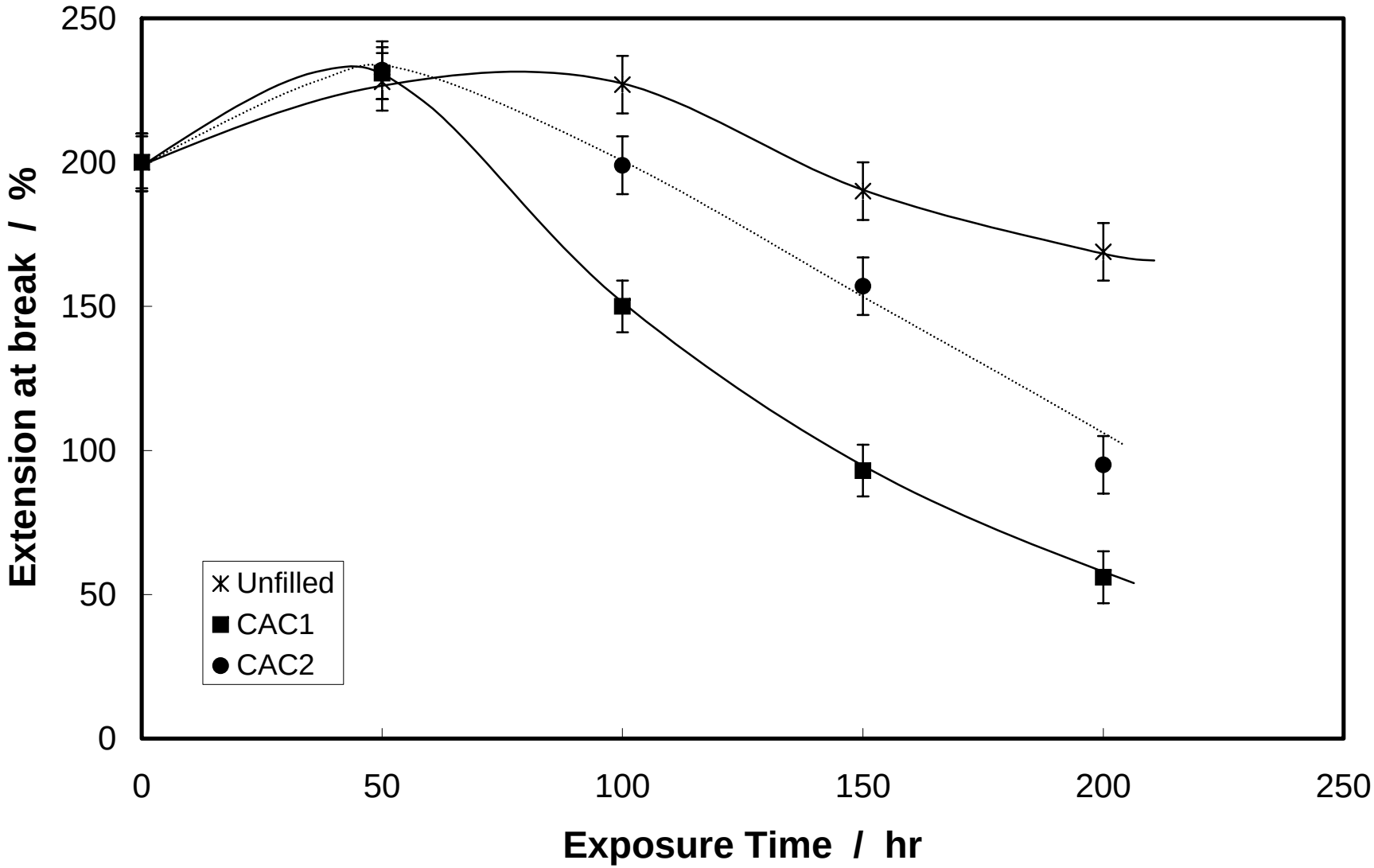

Figure 11: Area under the carbonyl peak in the FTIR spectra versus weathering time for PE films.